

# We are IntechOpen, the world's leading publisher of Open Access books Built by scientists, for scientists

6,900

Open access books available

186,000

International authors and editors

200M

Downloads

Our authors are among the

154

Countries delivered to

TOP 1%

most cited scientists

12.2%

Contributors from top 500 universities



WEB OF SCIENCE™

Selection of our books indexed in the Book Citation Index  
in Web of Science™ Core Collection (BKCI)

Interested in publishing with us?  
Contact [book.department@intechopen.com](mailto:book.department@intechopen.com)

Numbers displayed above are based on latest data collected.  
For more information visit [www.intechopen.com](http://www.intechopen.com)



## Segmentation Methods for Synthetic Aperture Radar

Shuang Wang  
*Xidian University, Xi'an,  
China*

### 1. Introduction

Synthetic aperture radar (SAR) image segmentation is a fundamental problem in SAR image interpretation. SAR images often contain non-texture object and texture object. Level set method, known as deformable model, is a powerful image segmentation technique. It can get accurate contours of non-texture object, but has poor performance in getting contours of texture object.

In recent years, parametric active contour model (snake), which was proposed by Kass in 1987 [1], has become one of the most studied techniques for image segmentation. The snake approach is based on deforming an initial contour or surface towards the boundary of the object to be detected. The deformation is obtained by minimizing a global energy designed such that its minimum is obtained at the boundary of the object. The energy is basically composed by a term which controls the smoothness of the deforming curve and another one which attracts it to the boundary. However, the classical active contour model presents several limitations. In particular, it is sensitive to initial contour placement, and most importantly, it can't handle topological changes of the curves during their evolution [2-4].

Geometric active contour model was subsequently proposed by Osher and Sethian in 1988 [5]. This model is based on the theory of curve evolution and geometric flows, which implemented using level set. Level set is designed to handle problems in which the evolving interfaces can develop sharp corners, change topology and become very complex. Level set approach has been widely applied to image processing [6-9].

SAR image segmentation is an important, challenging problem and a necessary first step in image analysis and interpretation. However, segmentation of distinct areas, such as city and river, is a challenging task due to their complex topologies. So we use level set approach to solve the topology problem. One class of image segmentation is object detection, where certain objects in the image are to be singled out. In this case, the image is basically divided into two sets: objects and background. Some non-texture objects in SAR image, such as river, ravine and railway, can be detected easily by level set method because of their distinctness with background and lack of texture. But in particular, objects in SAR image often contain texture, such as the city zone, which may cause considerable difficulties when applying level set approach. It makes the detection result too minute, and loses the consistency of objects. We would like to use level set method to get accurate contour of objects, whereas the consistency of objects is also needed. As a result, a new technique which could make level set method adaptable to detection of texture object is required.

Here, a new modified model of level set based on clonal selection algorithm [10] is proposed. We use clonal selection algorithm to choose some pixels near the contour, and then perform a neighborhood modification on these points of the level set function during its evolution. Their region texture information, supervising the modification process, is incorporated into the level set framework. This new method is particularly well adapted to segmentation of texture object of interesting. We illustrated the performance of the new method on SAR images. Furthermore, we compared our method with level set method and the modified model of level set based on standard genetic algorithm (SGA) in texture object detection result and image segmentation result. The experimental results show that incorporating region texture information into the level set framework, consistent texture objects are obtained, and accurate and robust segmentations can be achieved.

The level set method was devised by Osher and Sethian in 1988. The main idea is to describe a closed curve  $\Gamma(t)$  in the image plane as the zero level set of a higher dimensional function  $\Phi(x,t)$  in  $R^3$ .

$$\begin{cases} \Phi(x,t) > 0, & \text{if } x \text{ is inside } \Gamma(t) \\ \Phi(x,t) = 0, & \text{if } x \text{ is at } \Gamma(t) \\ \Phi(x,t) < 0, & \text{if } x \text{ is outside } \Gamma(t) \end{cases} \quad (1)$$

In numerical implementations, often regularity is imposed on  $\Phi$  to prevent the level set function to be too steep or flat near the interface. This is normally done by requiring  $\Phi$  being the signed distance function (SDF) to the interface.

$$\begin{cases} \Phi(x,t) = d(\Gamma(t),x), & \text{if } x \text{ is inside } \Gamma(t) \\ \Phi(x,t) = 0, & \text{if } x \text{ is at } \Gamma(t) \\ \Phi(x,t) = -d(\Gamma(t),x), & \text{if } x \text{ is outside } \Gamma(t) \end{cases} \quad (2)$$

Where  $d(\Gamma(t),x)$  denotes Euclidian distance between  $x$  and  $\Gamma(t)$ . We emphasize that requiring (2) is a technical processing to prevent instabilities in numerical implementations. Having defined the level set function, there is a one-to-one correspondence between the curve  $\Gamma$  and the function  $\Phi$ .

The evolution of  $\Phi(x,t)$  can be modeled as

$$\frac{\partial \Phi}{\partial t} + V|\nabla \Phi| = 0 \quad (3)$$

with a given  $\Phi(x,t=0)$ . At any instant, the position of  $\Gamma$  shall be given as the zero level set of evolving function  $\Phi$ . The speed function  $V$  depends on factors as the image gradient and local curvature.

The above motion equation (3) is a partial differential equation in a higher dimension than the original problem. Given the initial value, it can be solved by means of the following discretization and linearization.

$$\Phi(n+1) = \Phi(n) + \Delta \Phi(n) \quad (4)$$

$$\Delta\Phi(n) = \Delta t \cdot \delta_\varepsilon(\Phi(n)) \left[ \mu \operatorname{div} \left( \frac{\nabla\Phi(n)}{|\nabla\Phi(n)|} \right) - \nu + \lambda_1 (u_0 - c_1(n))^2 - \lambda_2 (u_0 - c_2(n))^2 \right] \quad (5)$$

In formula (4)  $n$  is the iterative time,  $\Phi(n)$  is the level set function value at time  $n$ , and  $\Delta\Phi(n)$  is the update quantity at time  $n$ . And  $\Delta t$  is the time step,  $\delta_\varepsilon(\Phi(n))$  is the Dirac measure,  $u_0$  is the image to be segmented,  $c_1(n)$  and  $c_2(n)$  are the averages of  $u_0$  outside and inside the curve  $\Gamma$  respectively, the constant  $\mu$  is length parameters,  $\nu$  is a correction term, and  $\lambda_1, \lambda_2$  are fixed parameters in formula (5). This implementation allows the function  $\Phi$  to automatically follow topological changes and corners during evolution [6, 7, 11, 12].

We all know that level set method can solve the complex topology problem and get accurate contour of objects. But it is lack of region information in its implementation, which makes its performance in getting contours of texture object not as well as we expect. So we must introduce region information into our work to supervise level set function during its evolution.

We perform modification repeatedly on the level set function in every iteration when the function is evolving. Clonal selection algorithm is used to choose pixels near the contour. According to the region texture information of each chosen point, we decide how to modify (positive or negative) and how much to modify (the parameter value). To effectively shift the contour and change topology, we do neighborhood modification instead of point modification. The principle of the modified model is shown in figure 1.

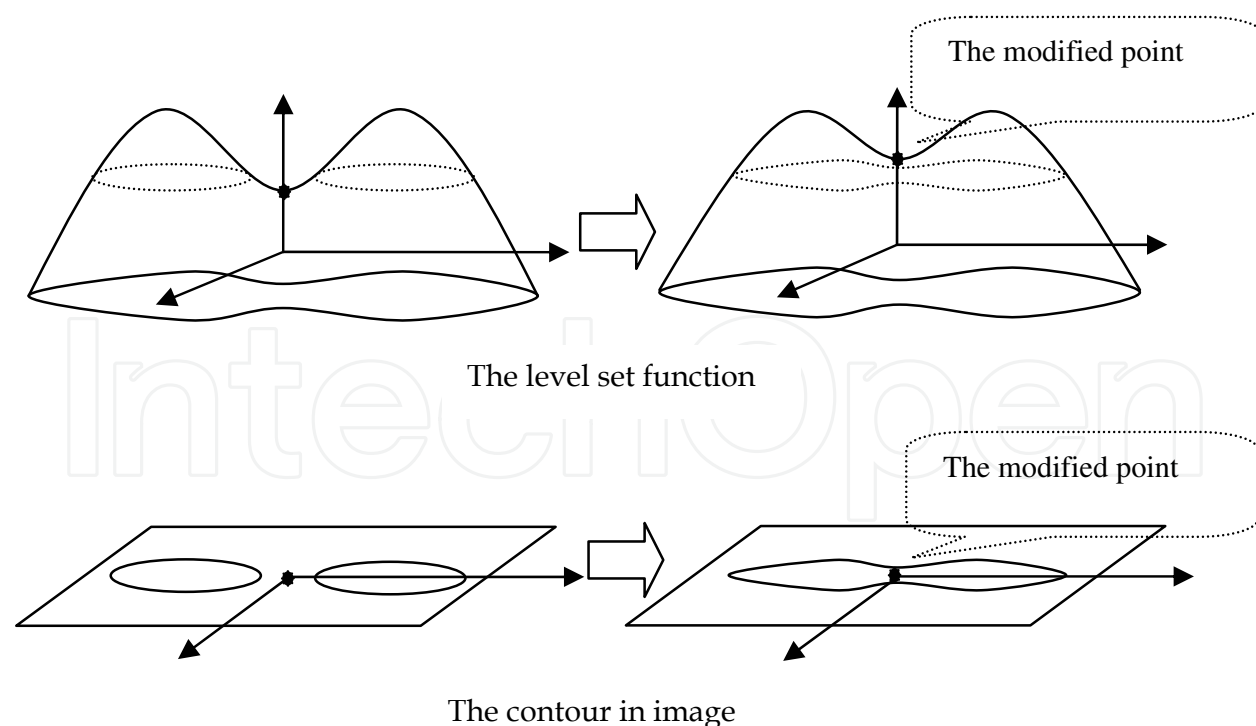


Fig. 1. The principle of the modified model, the point who has a region texture feature approximate to the object feature is given a positive modification. As a result, the nearby contours are connected and the object becomes more consistent.

To interpret the modification strategy, we note the area  $(i-\delta, i+\delta; j-\delta, j+\delta)$  as the  $\delta$  neighborhood of the pixel  $(i, j)$ , and note  $\Phi_{i,j}(\delta)$  as the  $\delta$  neighborhood of  $\Phi_{i,j}$ .

The modification of  $\Phi_{i,j}$  can be modeled as

$$\Phi_{i,j}(n+1, \delta) = \Phi_{i,j}(n, \delta) + \Delta\Phi_{i,j}(\delta) \quad (6)$$

where  $n$  is the iterative time,  $\Phi_{i,j}(n, \delta)$  is the level set function value of  $\delta$  neighborhood of pixel  $(i, j)$  at time  $n$ , and  $\Delta\Phi_{i,j}(\delta)$  is the modification value matrix. This implementation allows the function  $\Phi$  to follow region feature information automatically during modification. Here,  $\Delta\Phi_{i,j}(\delta)$  is defined as:

$$\Delta\Phi_{i,j}(\delta) = \sigma c_{i,j} T(\delta) \quad (7)$$

where  $\sigma$  is the global modification coefficient,  $c_{i,j}$  is the local modification coefficient of pixel  $(i, j)$ ,  $T(\delta)$  is the neighborhood template, which is expressed by a matrix.

We define  $d_n$  as the Euclidian distance between background  $n$  and the certain object in the feature space,  $d_{i,j}$  as the Euclidian distance between pixel  $(i, j)$  to be modified and the certain object in the feature space. Then, the parameter in formula (7) can be denoted as

$$c_{i,j} = -\frac{|d_{i,j} - d|}{d} \cdot (d_{i,j} - d) \quad (8)$$

$$T(\delta) = T(1) = \begin{bmatrix} 0.5 & 1 & 0.5 \\ 1 & 2 & 1 \\ 0.5 & 1 & 0.5 \end{bmatrix} \quad (9)$$

$$d = \min(d_1, d_2, \dots, d_n) / 2 \quad (10)$$

In order to make the modification steady, we introduce an inhibiting factor during the evolution of level set function and replace formula (4) by the following one.

$$\Phi_{i,j}(n+1) = \Phi_{i,j}(n) + h_{i,j} \Delta\Phi_{i,j}(n) \quad (11)$$

$$h_{i,j} = \lambda \left(1 - \frac{|d_{i,j} - d|}{d}\right) \quad (12)$$

where  $\lambda$  is the inhibiting coefficient.

In conclusion, the new method can be summarized as follows:

**Step 1.** Initialization.

- 1.1 Extract the texture feature. Sample the object and each background to calculate the mean feature value.
- 1.2 Initialize the level set function using SDF.
- 1.3 Initialize the parameters of clonal selection algorithm. The affinity is the level set function.
- 1.4 Initialize the generation  $n = 0$ . Initialize the maximal evolution generation.

**Step 2.** Evolve the level set function by formula (4) and (5).

**Step 3.** Modification.

3.1 Implement the clone and mutation operators, evaluate the affinity. And then select the points whose level set value are near zero level set.

3.2 Perform the modification by formula (6).

**Step 4.** Evolve the level set function by formula (11) for ten times.

**Step 5.** Let  $n = n + 1$ , return Step 3 until the maximal evolution generation is achieved.

### Experimental results

Three experiments have been carried out to test the efficiency of the proposed method. We regard the image segmentation problem as an object detection problem. That is to say, we detect texture and non-texture objects from the background separately, and then combine the detection results to obtain the final segmentation results.

In the following experiments, three different SAR images with size  $256 \times 256$  are used which contain both texture and non-texture objects. We combine the non-texture object detected by

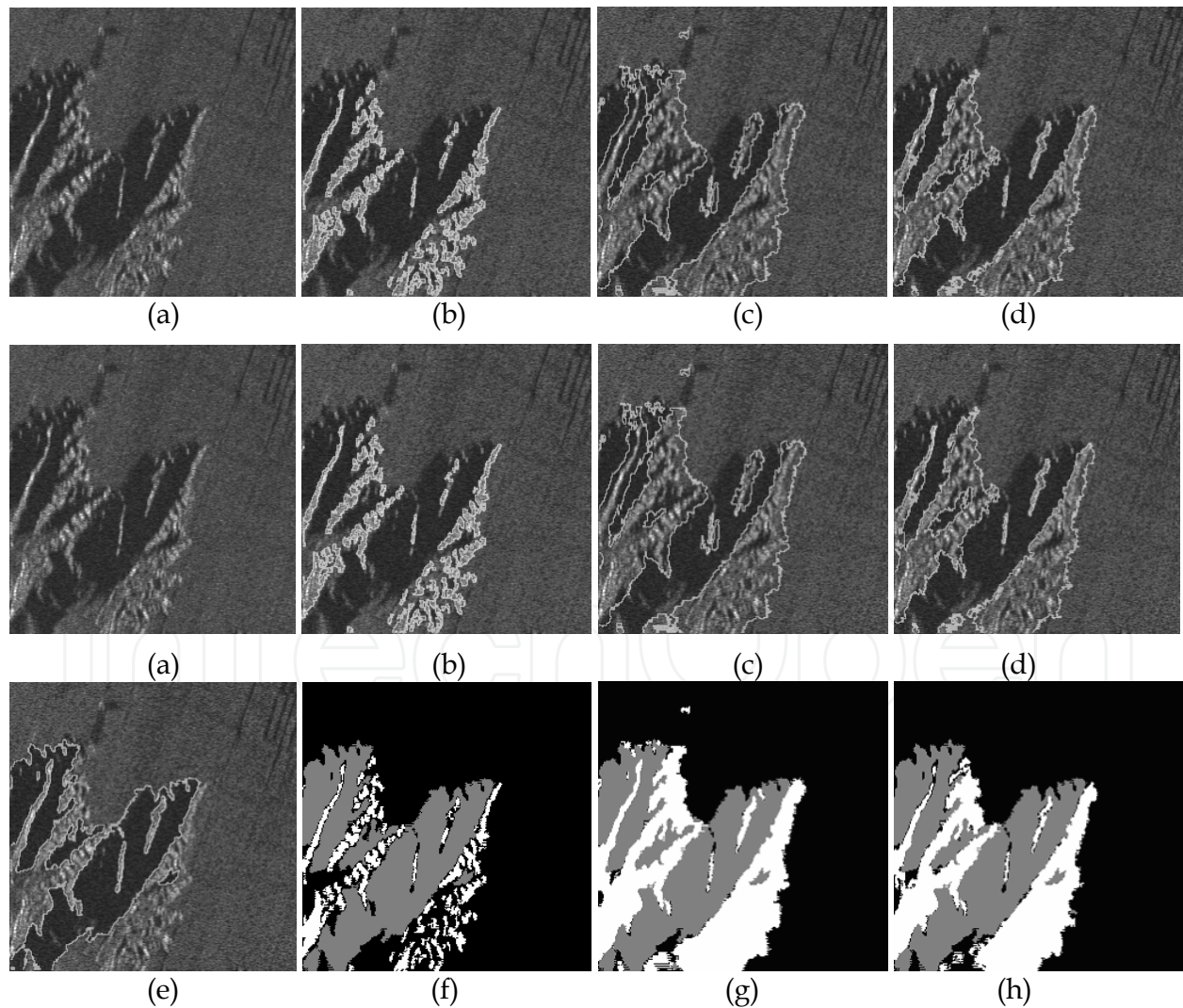


Fig. 2. SAR image experimental result 1, three methods were used and corresponding segmentation results were given.

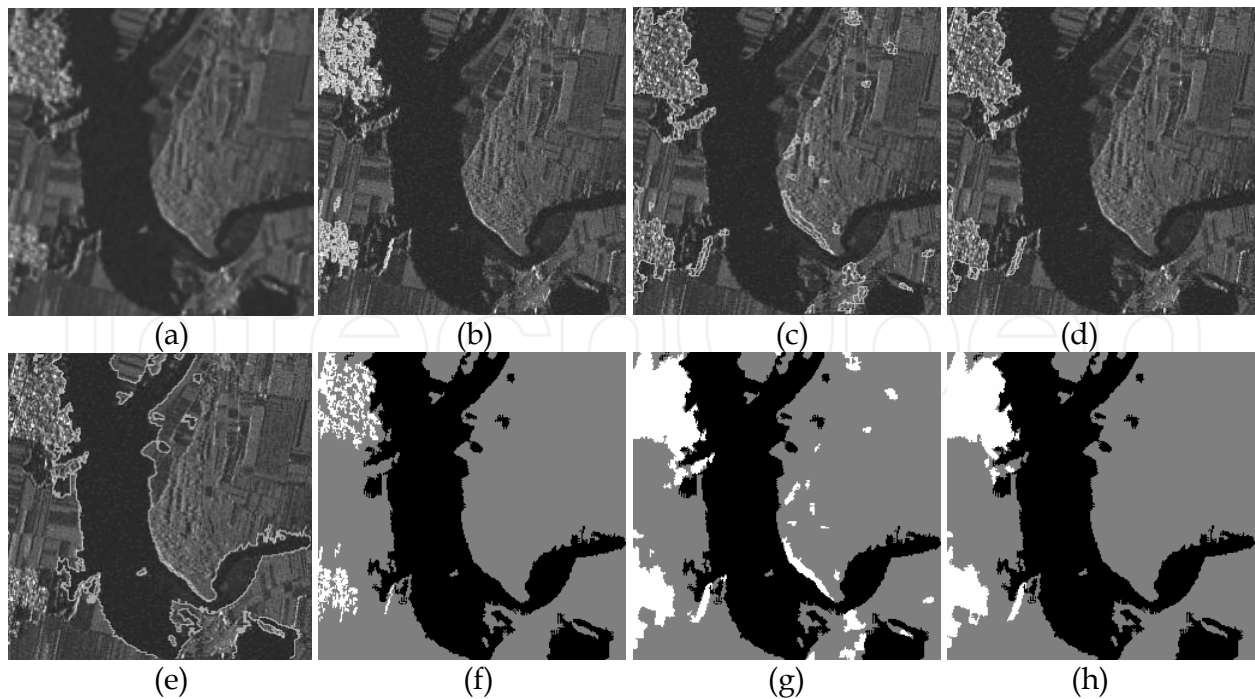


Fig. 3. SAR image experimental result 2, three methods were used and corresponding segmentation results were given.

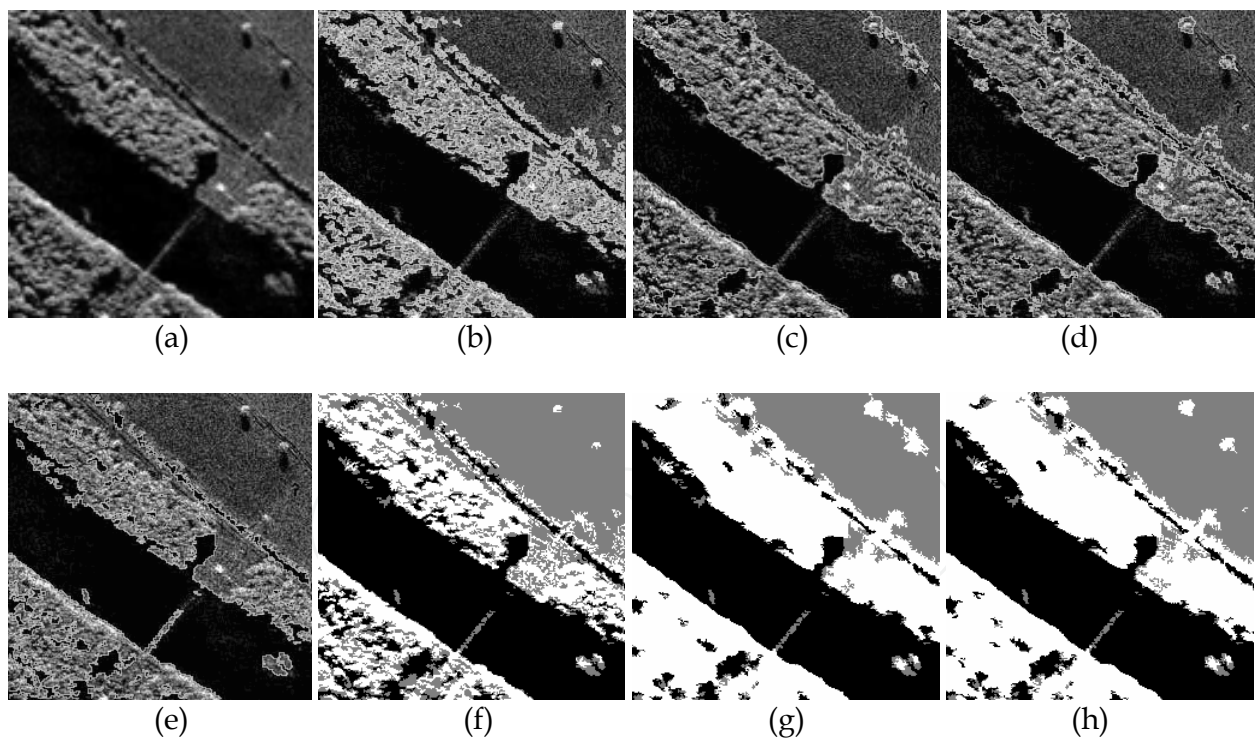


Fig. 4. SAR image experimental result 3, three methods were used and corresponding segmentation results were given.

level set method and the texture object detected by three different methods to obtain the segmentation results separately. First we compared our method with level set method without modification and the modified model of level set based on standard genetic algorithm (SGA) in texture object detection results. Then a further comparison of the three

methods was made in the final segmentation results. Feature vector with dimension 10 is extracted using the wavelet analysis. In clonal selection algorithm, a binary encoding scheme is used to represent the coordinate  $(i, j)$ . The initial antibody population size is 300 and the antibody length is 16. The clonal size is 5. The maximal evolution generation is 500. In SGA, the chromosome length, population size and the maximal evolution generation are as same as clonal selection algorithm. The experimental results are shown in figure 2 to 4.

In the experiments above, (a) is the original images, (b) is the texture object detection results by level set method, (c) is the texture object detection results by the modified model of level set based on SGA, (d) is our texture object detection results by the new modified model of level set method based on clonal selection algorithm, (e) is the non-texture object detection results by level set method, (f) is the segmentation results based on level set method, which is obtained by combine (b) and (e), (g) is the segmentation results by the modified model of level set based on SGA, which is obtained by combine (c) and (e), (h) is our finally segmentations by the new modified model of level set method based on clonal selection algorithm, which is obtained by combine (d) and (e).

From (b) to (d), we can see that (b) has the most accurate contour position, but it is too minute to be considered as a whole object, (c) is not accurate enough in contour and has some unfavorable modification, (d) is our result, which is more accurate than (c) and more consistent than (b). It is clear that the proposed method is efficient on the texture object detection. From (f) to (h), we give the corresponding segmentation results. From the object detection results acquired by three different methods referred above, it is clear that the proposed method is efficient on the texture object contour detection. And comparing the corresponding segmentation results, our method shows better performance. As a result, we can draw the conclusion that the modified model of level set based on clonal selection algorithm is more effective than the modified model of level set based on SGA and traditional level set methods in detecting texture objects, and therefore leads to better segmentation results.

We analyzed the modified model based on SGA and the modified model based on clonal selection algorithm especially. Two methods take the approximately same time, but show quite different performance. The modified model based on SGA is tend to be trapped in local optimization and induce excess or wrong modification, while the modified model based on clonal selection algorithm can jump out of local optimization and find proper points to be modified. As a result, we can draw the conclusion that the modified model of level set based on clonal selection algorithm is more effective than the modified model of level set based on SGA and traditional level set methods in detecting texture objects, and therefore leads to better segmentation results.

A modified model of level set based on clonal selection algorithm is formed by incorporating region texture information into the level set framework. The experiments show that this new method is of great efficiency in detecting consistent texture objects and proves to be particularly well adapted to accurate and robust segmentation of texture object of interest. If we choose our method to detect texture object and level set method to non-texture object, then accurate and robust segmentations can be achieved.

## 2. An improved watershed-based SAR image segmentation algorithm

In this section, we give another method about image segmentation which is based on the watershed algorithm because sometimes we need to keep the information such as boundaries. The watershed algorithm is a well established morphological segmentation tool, it commonly segments an image into a set of non overlapping regions. The watershed

algorithm has the advantage of region growing algorithm, the regions are spatially consistent, with boundaries forming a closed, connected set, it also makes use of edge information, as captured by the gradient surface. This kind of mathematical morphology segmentation method respectively considers light and dark image areas as the hills and valleys of an image landscape. To segment a given image the "landscape" is flooded, whereby water flows from high altitude areas (areas with high gray scale values) along lines of steepest descent until it reaches some regional minimum (low grayscale regions). The watersheds or catchment basins of the image are the draining areas of its regional minima. These areas are separated by lines called watershed lines.

Unfortunately, the segmentation produced by a naive application of the watershed algorithm is oftentimes inadequate: the image is usually over-segmented into a large number of minuscule regions. As a result, several extensions have been proposed in order to produce more natural image segmentation (e.g., hierarchical watersheds or region split/merge [14]). The most common remedy is to use markers for identifying relevant region minima (e.g., [15], [16] and [17]). By setting marker locations as the only local minima within the watershed image, the number of regions can be automatically controlled. Also, particular approach to finding and utilizing markers can be found in [18], [19] and [20], where researchers used a naive Bayes classifier to identify (i.e., classify) pixel groups as internal markers. Of course, these particular approach have good performance in controlling over-segmentation, but they are complex, low speed. So we show an improved watershed algorithm by referring to that in paper [17]. Its marker extraction method is one of the focal points of this paper.

Watershed segmentation is not effective for Synthetic Aperture Radar (SAR) images which are generally corrupted by coherent speckle noise, the image is usually over-segmented into a large number of minuscule regions due to speckle noise which tends to be amplified by the gradient operator. Gaussian filter is involved to smooth the image in many steps in our algorithm. Otsu algorithm is used to produce inner mark and external mark. It's unsupervised, low complexity and high speed. Then we use the mark to modify the gradient image of the SAR image. Additionally, rather than flooding the gradient image, we use the gradient image modified by the mark as input to the watershed algorithm.

First, we provide a brief overview of Gaussian filter. Next, we present the details of our algorithm. The following section presents experimental results carried out on a set of SAR images and discusses the significance of the results. The last section presents future research directions and concludes the paper.

Gaussian filter [21][22] has been intensively studied in image processing and computer vision. It's a kind of transform in frequency domain. Since frequency is directly related to rate of change, it is not difficult intuitively to associate frequencies in the Fourier transform with patterns of intensity variations in an image. It's that the slowest varying frequency component ( $u=v=0$ ) corresponds to the average gray level of an image. As we move away from the origin of the transform, the low frequencies correspond to the slowly varying components of an image while high frequencies correspond to detail, such as noise. A filter that attenuates high frequencies while "passing" low frequencies is called lowpass filter. A filter that has the opposite characteristic is appropriately called a highpass filter. We would expect a lowpass-filtered image to have less sharp detail than original because the high frequencies have been attenuated. Similarly, a highpass-filtered image would have less gray level variations in smooth areas and emphasized transitional gray-level detail. Such an image will appear sharper.

In this paper, Gaussian lowpass filter is used to suppress noise before extracting gradient image. So there will be less regional minima in the gradient image. It's a good help to control over-segmentation. It consists of the following steps[23]: (1) Multiply the input image by  $(-1)^{x+y}$  to center the transform; (2) compute  $F(u,v)$ , the DFT of the image; (3) Multiply  $F(u,v)$  by filter function  $H(u,v)$  (4) compute the inverse DFT of the result in (3); (5) Obtain the real part of the result in (4) (6) Multiply the result in (5) by  $(-1)^{x+y}$ . The Fourier transform of the output image after Gaussian lowpass filtering can be expressed as:

$$G(u,v) = H(u,v)F(u,v), H(u,v) = \exp(-(u^2 + v^2) / 2\sigma^2)$$

Otsu algorithm can be said to be adaptive to calculate the single threshold (for converting images to gray scale image) simple Efficient methods. Algorithm for the importation of gray image histogram analysis of histogram is divided into two parts, the method achieved a optimal threshold in many cases. Using the optimal segmentation threshold, we segment the SAR image into the target and background classes. In this paper, we extract mark from the gradient of the segmented image for watershed algorithm.

The Otsu algorithm is proposed on the principle of least squares. Firstly, its basic principle is to compute the inter-classes variance of each gray value, then segment the image according to the gray value with the maximum inter-classes variance value. Suppose the total pixel number of the image is  $M$ , the range of the gray values is  $[1, L]$ , the number of the pixel gray value  $i$  is  $m_i$ , the corresponding probability is  $P_i = m_i / M$ . Let  $C_0$  and  $C_1$  as the target and background classes respectively, which are divided by the value  $k$ . The gray value range of  $C_0$  is  $[1, k]$ , the gray value range of  $C_1$  is  $[k+1, L]$ . The gray value probability  $C_0$

is  $\omega_0 = \sum_{i=1}^k p_i$ , the gray value probability of  $C_1$  is  $\omega_1 = \sum_{i=k+1}^L p_i$ . In order to evaluate optimal

segmentation threshold, we shall introduce the following discriminant criterion measures (or measures of class separability) used in the discriminant.

Analysis. Let  $\sigma_w^2$ ,  $\sigma_B^2$  and  $\sigma_T^2$  as the within-class variance, between-classes variance and total variance of levels respectively.

$$\lambda = \frac{\sigma_B^2}{\sigma_w^2}, \quad \kappa = \frac{\sigma_T^2}{\sigma_w^2}, \quad \eta = \frac{\sigma_B^2}{\sigma_T^2}$$

there  $\sigma_w^2 = \omega_0 \sigma_0^2 + \omega_1 \sigma_1^2$ ,  $\sigma_B^2 = \omega_0 (\mu_0 - \mu_T)^2 + \omega_1 (\mu_1 - \mu_T)^2 = \omega_0 \omega_1 (\mu_0 - \mu_1)^2$

$$\sigma_T^2 = \sigma_w^2 + \sigma_B^2, \quad \mu_T = \sum_{i=0}^{L-1} iP_i, \quad \mu_t = \sum_{i=0}^t iP_i, \quad \mu_0 = \frac{\mu_t}{\omega_0}, \quad \mu_1 = \frac{\mu_T - \mu_t}{1 - \omega_0}$$

the optimal segmentation threshold that maximizes  $\eta$ , or equivalently maximizes  $\sigma_B^2$  is  $t^* = \arg \max_{t \in G} \sigma_B^2$ .

The watershed algorithm was originally developed by Lantuéjoul [25] and is extensively described together with its many applications by Beucher and Meyer [26]. Since its original development with grey-scale images [25] it has been extended to a computationally efficient form (using FIFO queues) [27] and applied to color images [28]. The main advantages of the watershed method over other previously developed segmentation methods are [26]:

- The resulting boundaries form closed and connected regions. Traditional edge based techniques most often form disconnected boundaries that need post-processing to produce closed regions.
- The boundaries of the resulting regions always correspond to contours which appear in the image as obvious contours of objects. This is in contrast to split and merge methods where the first splitting is often a simple regular sectioning of the image leading sometimes to unstable results.
- The union of all the regions form the entire image region.

Direct application of the watershed segmentation algorithm leads to over-segmentation due to noise and other local irregularities of the gradient. A practical solution to this problem is to limit the number of allowable regions by incorporating a preprocessing stage designed to bring additional knowledge into segmentation procedure. To be effective these methods require object markers.

Instead of using the image directly, watershed transform uses a gradient image extracted from the original image. The initial stage of any watershed segmentation method is therefore to produce a gradient image from the actual image. So we need to extract gradient image of original image by "prewitt" operator. Soille's algorithm use markers to modifies it using morphological reconstruction so it only has regional minima when internal image and external image are nonzero. A marker is a connected component belonging to an image. In this paper, there are two kinds of markers, an internal markers and external markers, marker based watershed was transposed to marker selection problem. In this paper, internal markers is defined in this case as (1) a region that is surrounded by points of higher 'altitude'; (2) such that the points in the region form a connected component; and (3) in which all the points in the region form a connected component have the same gray level value.

However, Soille's algorithm is useless for SAR image segmentation, coherent speckle noise and texture information also cause so much over-segmentation. So we propose our improved algorithm. To obtain fewer internal markers, Firstly, we segment the SAR image using Otsu method. Smoothing the initial segmentation by Gaussian filter is also necessary, because it can reduce small regions which will produce redundant markers. Secondly, we obtain the gradient of the segmentation by gradient operator and we smooth it again using low pass filter to emphasize the significant gradient within the image and reduce the gradient caused by coherent speckle noise or other minor structures, such as texture in SAR images. Thirdly, we select internal marker from the smoothed gradient image. Selecting internal marker is to find regional minima in the gradient image, regional minima are connected components of pixels with a constant intensity value, and whose external boundary pixels all have a higher value. The value is called fall threshold. The higher fall threshold, the fewer the number of region. One marker per region is necessary since there will be a one-to-one correspondence between the marker and segments of the final partition. The external markers are the watershed of internal marker image which effectively partition the image into regions, with each region containing a single internal marker. At last, we obtain the gradient of original SAR image by gradient operator, the gradient image is modified by internal marker and external marker. The watershed algorithm applied to the modified gradient. The markers controlled the number of regions, and the original gradient image insures that the boundaries of segmentation result are accurate.

The program in detail is shown in Fig 1.

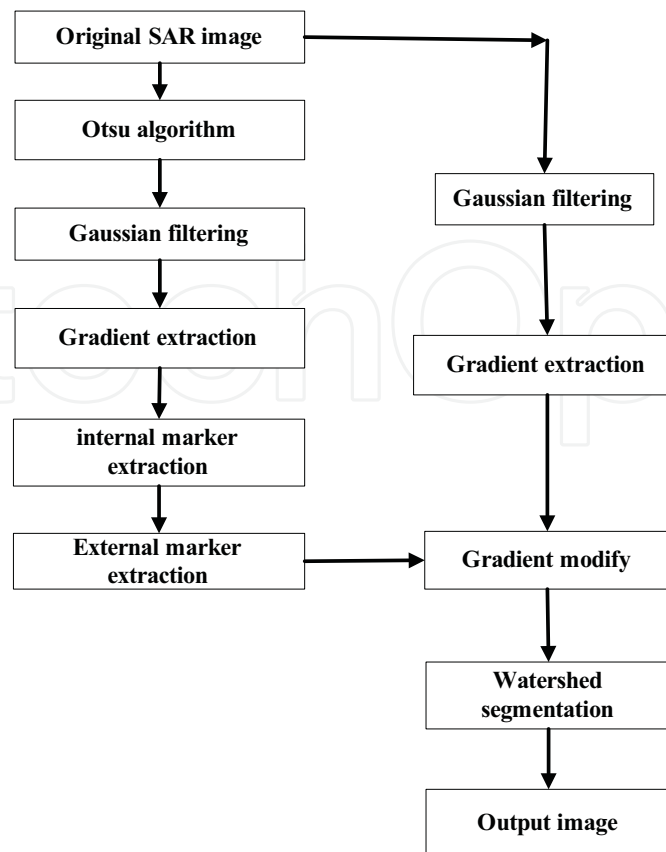


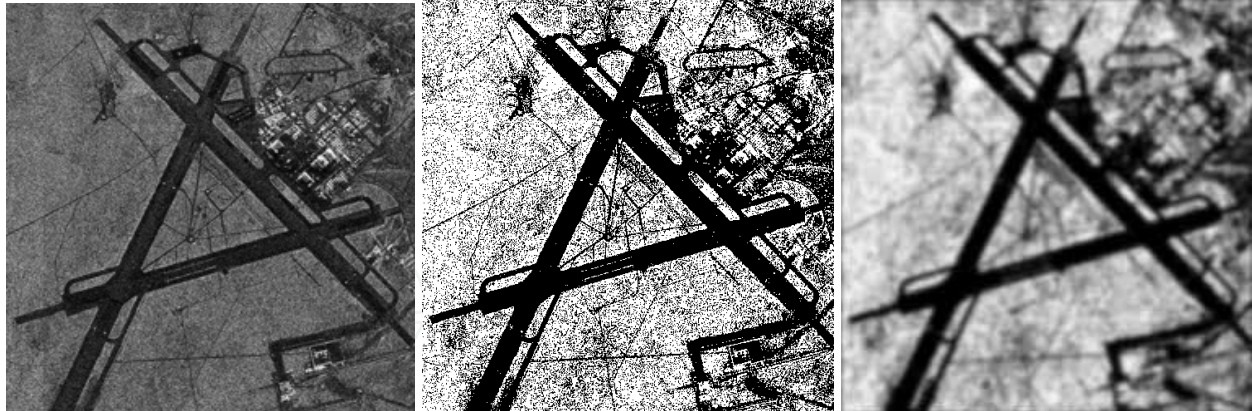
Fig. 1

### Experimental results

The proposed algorithm has been executed on a set of SAR images. The test images used in the experiment are shown in Fig.1a to Fig.4a. The segmentation results of our proposed algorithm, watershed algorithm and marker-controlled watershed algorithm with different threshold are shown in (d)- (i) Fig.1. to Fig.4. The average number of block of the segmentation results of different methods are shown in Table.1. In addition, we use different fall thresholds in marker-controlled watershed and our algorithm. In comparison with the initial segmentation results of watershed algorithm, the edges obtained by the proposed method are quite close to the real edges. From Table.1, we can see that the block number of our algorithm are lesser than that of watershed method and the algorithm of [17].

Original image		Watershed algorithm	Algorithm of [5]			Our algorithm		
			1	10	20	30	40	50
SAR image I	Block number	3187	3187	1166	611	230	84	30
SAR image II	Block number	4932	4932	3096	2475	22	6	4
SAR image III	Block number	2121	2121	1313	1107	57	33	19
SAR image IV	Block number	1434	1434	565	358	110	71	47

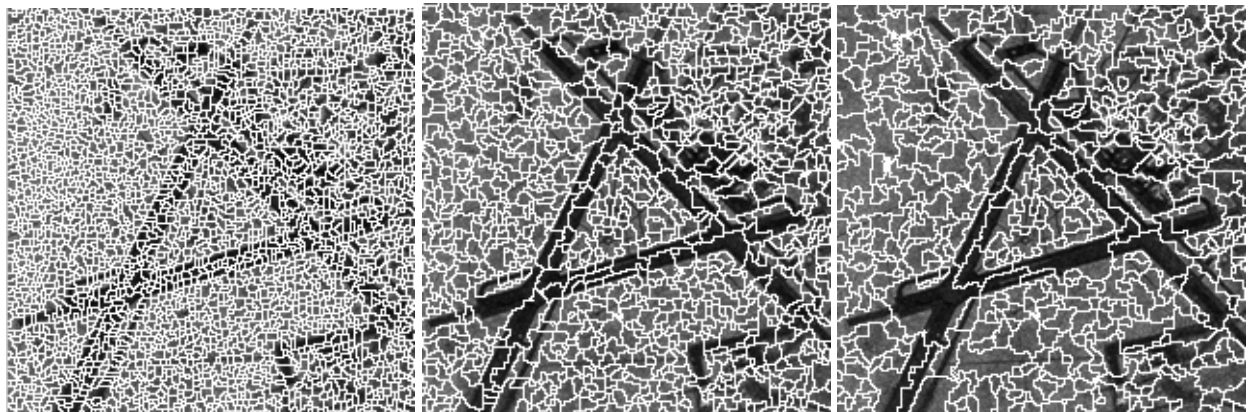
Table1. experiment result



(a) original SAR image

(b) watershed segmentation

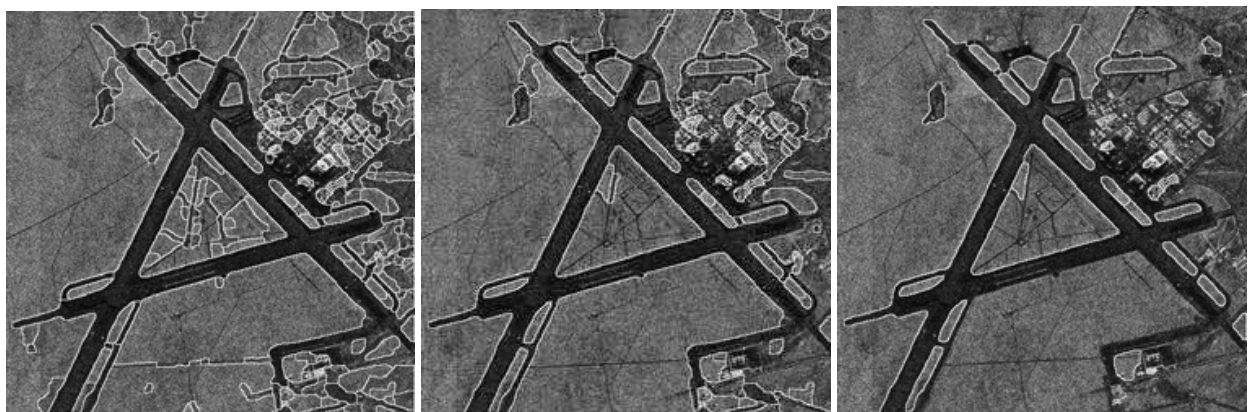
(c) final result



(d) watershed

(e) marker-controlled watershed (threshold 10)

(f) marker-controlled watershed (threshold 20)



(g) our algorithm (threshold 30)

(h) our algorithm (threshold 40)

(i) our algorithm (threshold 50)

Fig. 2.

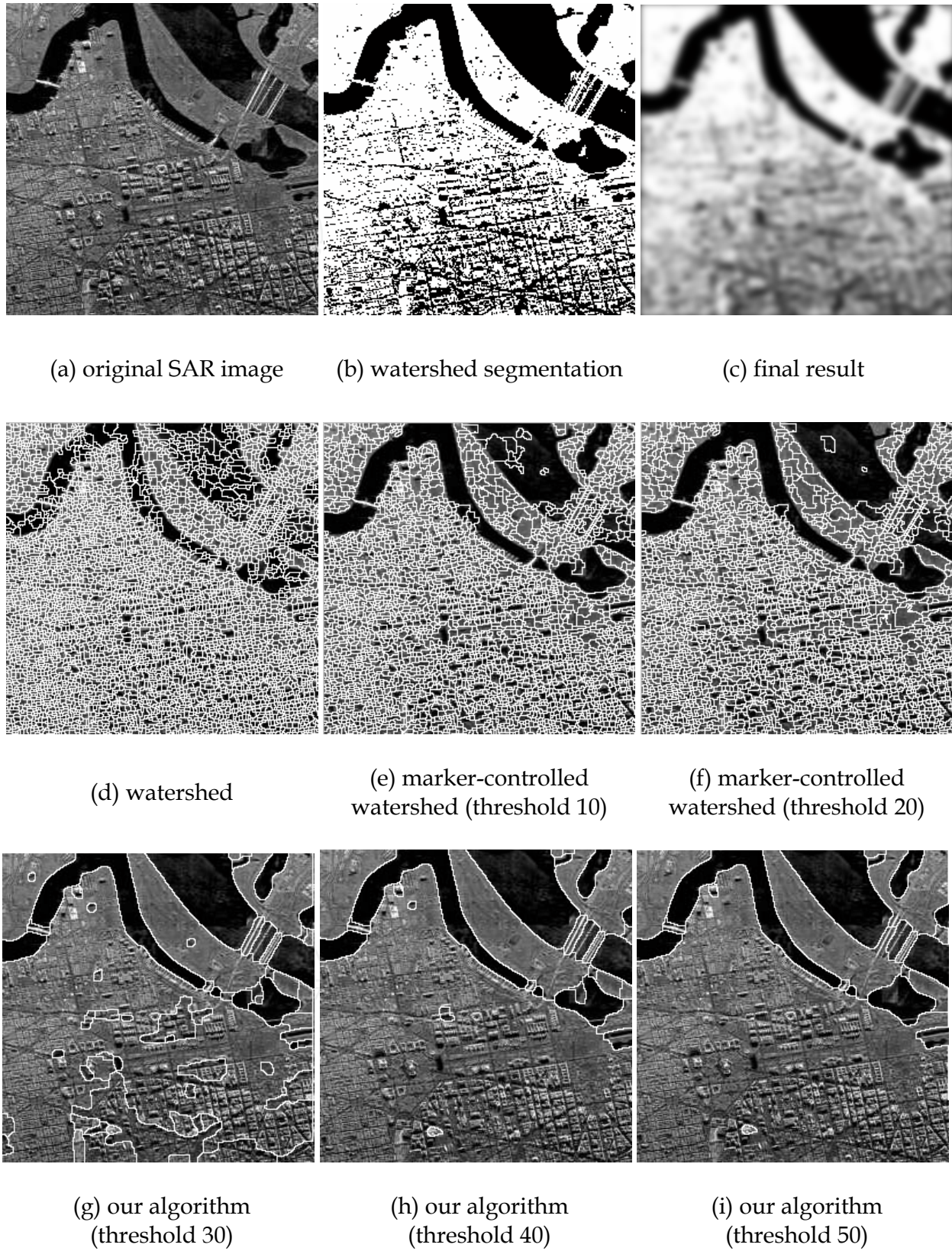


Fig. 3

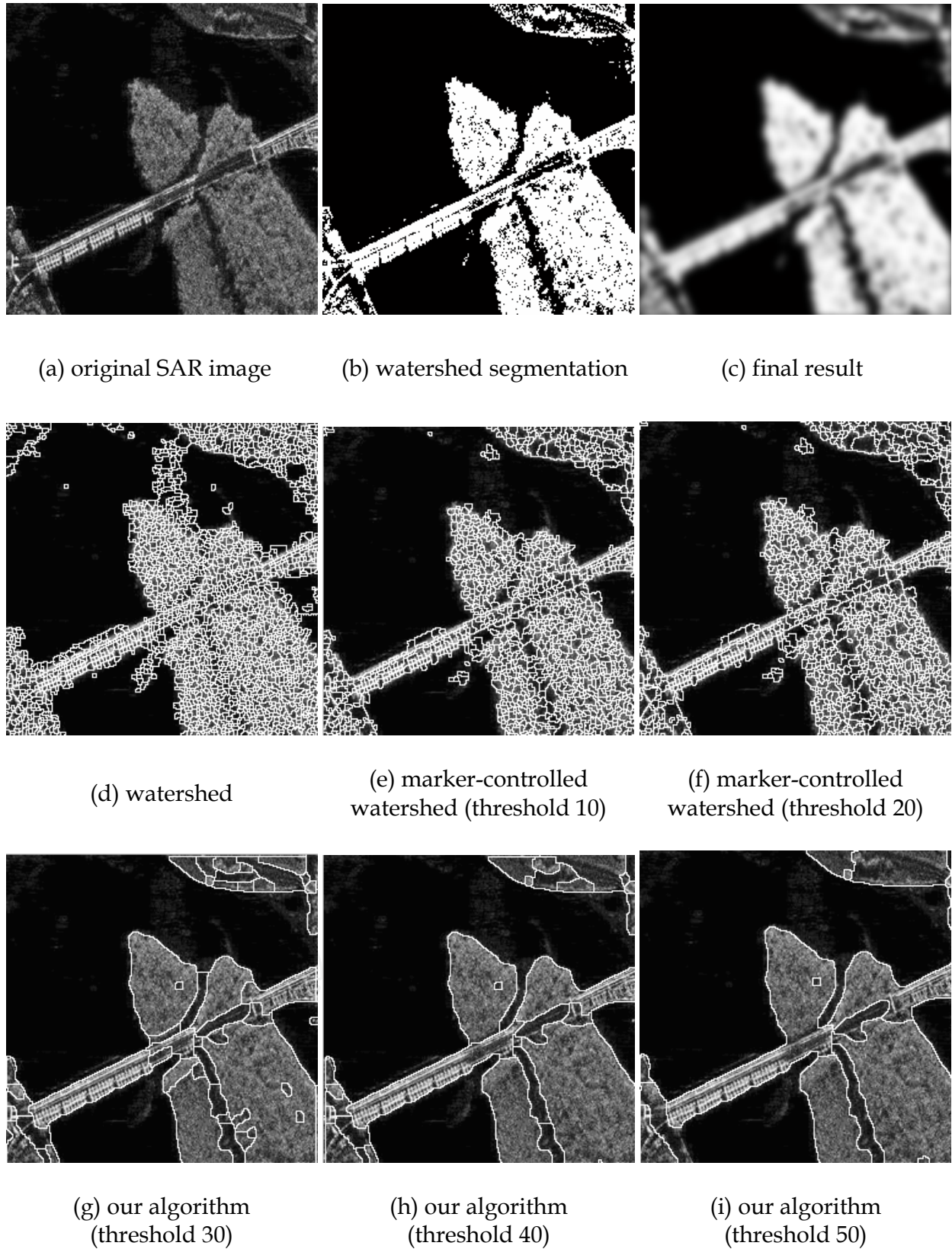


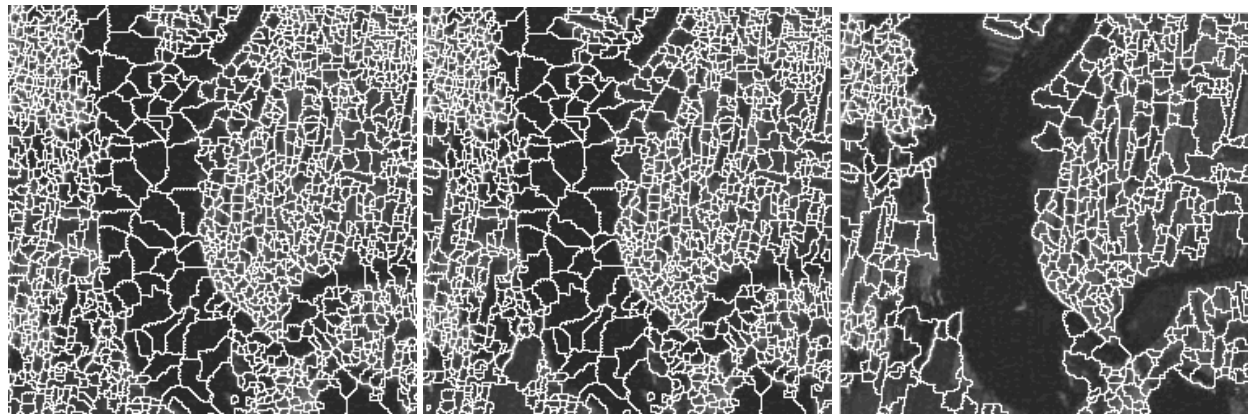
Fig. 4



(a) original SAR image

(b) watershed segmentation

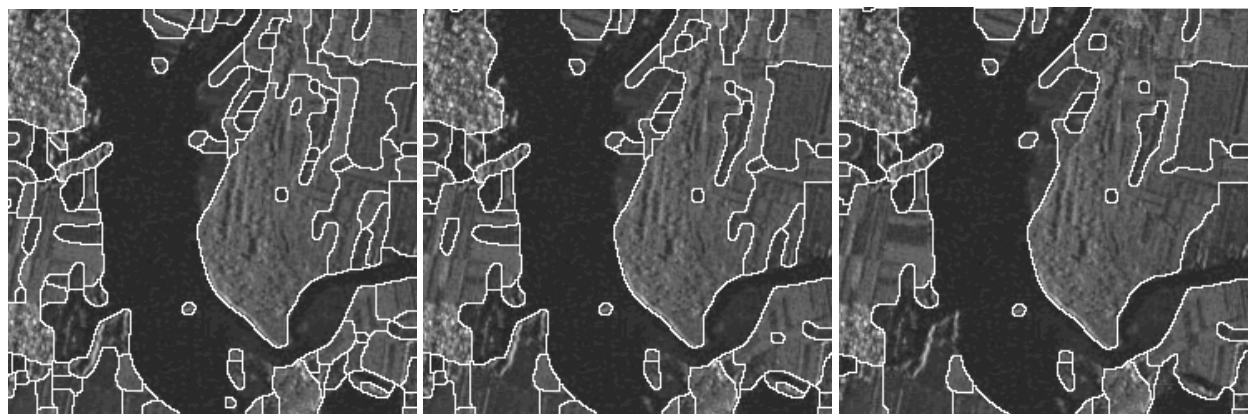
(c) final result



(d) watershed

(e) marker-controlled watershed (threshold 10)

(f) marker-controlled watershed (threshold 20)



(g) our algorithm (threshold 30)

(h) our algorithm (threshold 40)

(i) our algorithm (threshold 50)

Fig. 5

An algorithm for improving the quality of the SAR images segmentation based on watershed was proposed. Finding markers is the focal points of this paper. We use markers to solve the over-segmentation of watershed. Otsu method has been used during marker extraction. By using Gradient image modified by the markers as the input of watershed, the number of regions can be automatically controlled, more natural image segmentation can be produced. Our results show that the proposed technique is robust to SAR images segmentation.

However, further research is necessary to concentrate on finding markers, such as some texture feature method can be used. These methods may be more effective to SAR image segmentation since they contain more texture information.

### **3. SAR images segmentation based on undecimated wavelet transform and mean shift**

Synthetic Aperture Radar (SAR) has been a useful tool in domains such as disaster detection, cartography and crop monitoring. The images usually have inferior illumination quality mainly due to different type of environmental distributions. So the segmentation of different land covered regions is an important but difficult step in SAR image processing. It is also significant to understand how information changes over different scales of SAR image. Undecimated wavelet transform is good in describing a scene in terms of the scale; hence we choose this transformation's sub-band as features.

Based on feature space analysis, there are many image segmentation algorithms, which map the pixels into a feature space and cluster, with each cluster delineating a homogeneous region in the image. Although the popular clustering algorithms such as FCM and K-means are simple and fast, they have a major drawback: they seek to minimize the trace of the within-group dispersion matrix and consequently can only generate spherical boundaries. In contrast, mean shift can avoid this drawback. It does not assume any prior shape on data clusters and can handle arbitrary feature spaces.

Besides, texture is an important characteristic used to identify objects or regions of interest in a SAR image. Those textural properties of a SAR image are likely to provide valuable information for analysis, where different object regions are treated as different texture classes. There are numerous texture analysis methods over the past decades. Tuceryan and Jain[30] identifies five major categories of features for texture identification: statistical, geometrical, structural, model-based, and signal processing features. And many people use those methods to obtain supervised segmentation. In other words, many classical segmentation methods can not segment SAR images successfully without prior knowledge of the number of clusters. Fortunately, mean shift can meet our needs, which can determine the number of cluster automatically.

This SAR image segmentation algorithm include four parts: extracting features using undecimated wavelet decomposition; selecting suitable feature subset; filtering feature subset using a Kuwahara filter; at last, applying mean shift algorithm to gain final results. This algorithm does not require prior knowledge of the number of clusters, and does not constrain their shapes.

Discrete wavelet transform (DWT) is a popular tool for feature extraction. Its ability to repeatedly decompose an image in the low-frequency channels makes it ideal for image analysis since the lower frequencies tend to dominate real images. Decimation of the wavelet coefficients is an intrinsic property of the discrete wavelet transform

(DWT). Nevertheless, the decimation is causing shift variance of the wavelet transform. The shift variance means that the DWTs of a signal and its shifted version are not the same. This is because there are downsampling in pyramid discrete wavelet transform. Consequently, we can hardly obtain accurate and robust segmentation using wavelet coefficients as features. Fortunately, undecimated wavelet transform (UWT) can solve this problem.

Undecimated wavelet transform (UWT) is known redundant, shift-invariant and stationary. The number of the wavelet coefficients does not shrink between the transform levels. This additional information can be very useful for the better analysis and understanding of the image properties. Undecimated wavelet transform (UWT)  $W$  using the filter bank  $(h, g)$  of a 1D signal  $c_0$  leads to a set  $W = \{w_1, \dots, w_J, c_J\}$  where  $w_j$  are the wavelet coefficients at scale  $j$  and  $c_J$  are the coefficients at the coarsest resolution. The passage from one resolution to the next one is obtained using the "à trous" algorithm:

$$c_{j+1}[l] = (\bar{h}^{(j)} * c_j)[l] = \sum_k h[k]c_j[l + 2^j k] \quad (1)$$

$$w_{j+1}[l] = (\bar{g}^{(j)} * c_j)[l] = \sum_k g[k]c_j[l + 2^j k] \quad (2)$$

Where  $h^{(j)}[l] = h[l]$  if  $l / 2^j$  is an integer and 0 otherwise. For example, we have

$$h^{(1)} = (\dots, h[-2], 0, h[-1], 0, h[0], 0, h[1], 0, h[2], \dots) \quad (3)$$

The reconstruction is obtained by

$$c_j[l] = \frac{1}{2} [(\tilde{h}^{(j)} * c_{j+1})[l] + (\tilde{g}^{(j)} * w_{j+1})[l]] \quad (4)$$

The filter bank  $(h, g, \tilde{h}, \tilde{g})$  needs only to verify the exact reconstruction condition:

$$H(z^{-1})\tilde{H}(z) + G(z^{-1})\tilde{G}(z) = 1 \quad (5)$$

The à trous algorithm can be extended to 2D, by:

$$\begin{aligned} c_{j+1}[k, l] &= (\bar{h}^{(j)} \bar{h}^{(j)} * c_j)[k, l] \\ \omega_{j+1}^1[k, l] &= (\bar{g}^{(j)} \bar{h}^{(j)} * c_j)[k, l] \\ \omega_{j+1}^2[k, l] &= (\bar{h}^{(j)} \bar{g}^{(j)} * c_j)[k, l] \\ \omega_{j+1}^3[k, l] &= (\bar{g}^{(j)} \bar{g}^{(j)} * c_j)[k, l] \end{aligned} \quad (6)$$

where  $hg * c$  is the convolution of  $c$  by the separable filter  $hg$  (i.e. convolution first along the columns by  $h$  and then convolution along the rows by  $g$ ). At each scale, we have three wavelet images,  $\omega^1, \omega^2, \omega^3$ , and each has the same size as the original image. The redundancy factor is therefore  $3(J - 1) + 1$

This procedure is implemented by the similar filter bank as wavelet transform just without down sampling performance. In Fig.1, a typical filter bank of undecimated wavelet transform is shown.

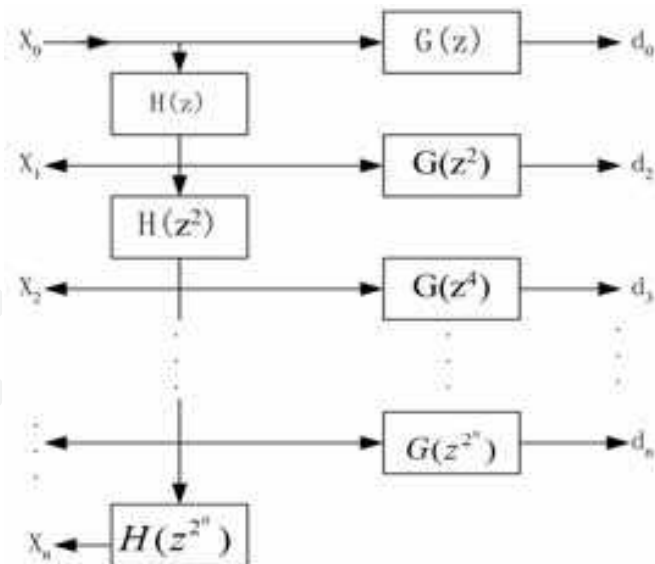


Fig. 1. Filter bank of undecimated wavelet transform

Accordingly, the undecimated wavelet decomposition provides robust texture features at the expense of redundancy. We use undecimated coefficients as features for SAR image analysis.

The simple combination of these features with each other is usually not suitable in SAR image segmentation due to the resulting redundancy and the additive computation complexity. Accordingly, it is necessary to find the most suitable feature subset for SAR image segmentation. This procedure is always considered as an optimization problem, and sequential forward selection (SFS) algorithm can be used.

Sequential forward selection is a traditional feature selection algorithm. It starts with an empty feature subset. On each iteration, exactly one feature is added to the feature subset. To determine which feature to add, the algorithm tentatively adds to the candidate feature subset one feature that is not already selected and tests the criterion function built on the tentative feature subset. The feature that results in the highest value of criterion function is definitely added to the feature subset. In experiments, the termination condition is the maximal iterations. In this paper, we choose Euclidean distance as criterion function and use the coarsest resolution's coefficient as first selected feature.

To avoid noise in SAR, we filter those selected features through a Kuwahara filter. Owing to the mask which contain edges having bigger variance, Kuwahara filter [7] is designed as Fig.2. Calculate variances in those four masks respectively, and then change the center feature with features' mean in which mask has the smallest variance. The realization step is as follows

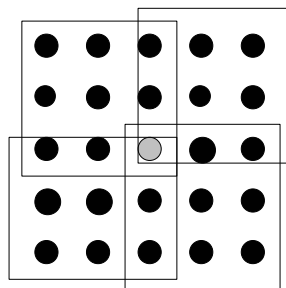


Fig. 2. Kuwahara filter

- Calculate variances in four masks respectively.
- Choose the mask which has the smallest variance, and calculate features' mean in this mask.
- Change center feature with this mean.
- Carry on this procedure to every feature.

Mean shift was proposed in 1975 by Fukunaga and Hostetler and largely forgotten until Dorin Comaniciu's paper[34]rekindled interest in it. Dorin Comaniciu proved that the mean shift procedure is an extremely versatile tool for feature space analysis and can provide reliable solutions for many vision tasks. It tries to obtain the modes of the probability density function of the feature space, using a nonparametric estimate of the density function. And the number of clusters is obtained automatically by finding the centers of the densest regions in the feature space.

To estimate the density function, we use kernel density estimation (known as the Parzen window technique in pattern recognition literature[33]). Assuming the reduced feature dimension is  $d$  and a set of point  $X = \{X_1, \dots, X_N\} \subset \mathcal{R}^d$  drawn from a probability density  $f(x)$ . Then, the multivariate kernel density estimate obtained with kernel function  $K(x)$  and window radius  $h$ , computed in the point  $x$  is defined as:

$$\hat{f}(x) = \frac{1}{nh^d} \sum_{i=1}^n K\left(\frac{x-x_i}{h}\right) \quad (7)$$

Where the kernel function  $k(x)$  can be different types such as Gaussian kernel, unit kernel, Epanechnikov kernel and so on. Using Epanechnikov kernel, the density estimator (7) can be rewritten as

$$\hat{f}_{h,k}(x) = \frac{C_{k,d}}{nh^d} \sum_{i=1}^n k\left(\left|\frac{x-x_i}{h}\right|^2\right) \quad (8)$$

Where  $C_{k,d}$  is the volume of unit  $d$ -dimensional sphere.

The density gradient estimator is obtained as gradient of the density estimator by exploiting the linearity

$$\begin{aligned} \hat{\nabla} f_{h,k}(x) &\equiv \hat{\nabla} f_{h,k}(x) = \frac{2C_{k,d}}{nh^{d+2}} \sum_{i=1}^n (x-x_i)k'\left(\left|\frac{x-x_i}{h}\right|^2\right) \\ &= \frac{2C_{k,d}}{nh^{d+2}} \left[ \sum_{i=1}^n g\left(\left|\frac{x-x_i}{h}\right|^2\right) \right] \left[ \frac{\sum_{i=1}^n x_i g\left(\left|\frac{x-x_i}{h}\right|^2\right)}{\sum_{i=1}^n g\left(\left|\frac{x-x_i}{h}\right|^2\right)} - x \right] \end{aligned} \quad (9)$$

Where  $g(x) = -k'(x)$ . And the second term is the mean shift

$$m_{h,G}(x) = \frac{\sum_{i=1}^n x_i g\left(\left|\frac{x-x_i}{h}\right|^2\right)}{\sum_{i=1}^n g\left(\left|\frac{x-x_i}{h}\right|^2\right)} - x \quad (10)$$

I.e., the difference between the weighted mean, using the kernel  $G$  for weight, and  $x$ , the center of the kernel (window). This vector thus always points toward the direction of maximum increase in the density. Since the mean shift vector is aligned with the local gradient estimate, it can define a path leading to a stationary point of the estimated density. Denote by  $\{y_j\}_{j=1,2,\dots}$  the sequence of successive locations of the kernel  $G$ , where, from (10),

$$y_{j+1} = \frac{\sum_{i=1}^n x_i g\left(\left|\frac{x-x_i}{h}\right|^2\right)}{\sum_{i=1}^n g\left(\left|\frac{x-x_i}{h}\right|^2\right)} \quad j=1,2,\dots \quad (11)$$

Is the weighted mean at  $y_j$  computed with kernel  $G$  and  $y_1$  is the center of the initial position of the kernel. The corresponding sequence of density estimates computed with  $K$ ,  $\{\hat{f}_{h,K}(j)\}_{j=1,2,\dots}$ , is given by

$$\hat{f}_{h,K}(j) = \hat{f}_{h,K}(y_j) \quad j=1,2,\dots \quad (12)$$

Dorin Comaniciu[34] proved that if the kernel  $K$  has a convex and monotonically decreasing profile, the sequences  $\{y_j\}_{j=1,2,\dots}$  and  $\{\hat{f}_{h,K}(j)\}_{j=1,2,\dots}$  converge and  $\{\hat{f}_{h,K}(j)\}_{j=1,2,\dots}$  is monotonically increasing.

An image is typically represented as a two-dimensional lattice of  $p$ -dimensional vectors (features). The space of the lattice is known as the spatial domain, while the features are represented in the range domain. In image analysis problem, mean shift incorporate this spatial coordinates of a feature in to its feature space representation. Thus, the multivariate kernel is defined as the product of two radially symmetric kernels and the Euclidean metric allows a single bandwidth parameter for each domain

$$K_{h_s^2, h_r^p}(x) = \frac{C}{h_s^2 h_r^p} k\left(\left|\frac{x^s}{h_s}\right|^2\right) k\left(\left|\frac{x^r}{h_r}\right|^2\right) \quad (13)$$

Where  $x^s$  is the spatial part,  $x^r$  is the range part of a feature vector,  $k(x)$  the common profile used in both two domains,  $h_s$  and  $h_r$  the employed kernel bandwidths, and  $C$  the corresponding normalization constant.

Using gray level of the image as features, this method performs well in natural image segmentation. But we proved that it could not segment SAR images directly, as there were too many texture regions which could not be described effectively just using gray level features. To solve this problem, mean shift algorithm is applied to undecimated wavelet coefficients features. In this feature space, the mean shift vector is aligned with the local gradient estimate, it can define a path leading to the local maxima of the density, i.e. the detected modes. This procedure is applied recursively to every point in the feature space, and the number of clusters present in the feature space is automatically determined by the number of significant modes. This algorithm need to be setted only the bandwidth parameter  $h = (h_s, h_r)$ , which, by controlling the size of the kernel, determines the resolution of the mode detection. In this paper, we set it just through experiments.

Let  $x_i$  and  $z_i, i = 1, \dots, n$ , be the d-dimensional input and filtered image features. For each pixel,

1. Initialize  $j = 1$  and  $y_{i,1} = x_i$ .
2. Compute  $y_{i,j+1}$  according to (11) until convergence,  $y = y_{i,c}$ .
3. Store all the information about the d-dimensional convergence point in  $z_i$ , i.e.,  $z_i = y_{i,c}$ .
4. Delineate in the joint domain the clusters  $\{C_p\}_{p=1..m}$  by grouping together all  $z_i$  which are closer than  $h_s$  in the spatial domain and  $h_r$  in the range domain, i.e., concatenate the basins of attraction of the corresponding convergence points.
5. For each  $i = 1, \dots, n$ , assign  $L_i = \{p | z_i \in C_p\}$ .
6. Eliminate spatial regions containing less than M pixels.

The algorithm has several steps as follows:

1. Extract features using undecimated wavelet transform.
2. Select suitable feature subset using SFS algorithm.
3. For all reserve features, filter them through a Kuwahara filter.
4. Use mean shift in feature space to gain the segmentation result.

### Experimental results

The proposed method has been applied to several SAR images as Fig.3.(a) and Fig.4.(a) with  $(h_s, h_r, M) = (5, 0.2, 20)$ . The segmentation of these image presented in Fig.3.(d) and Fig.4.(d) are satisfactory.

We compare our algorithm with Salari E's [36]. Salari E developed an algorithm that segments image using hierarchical wavelet decomposition. In his method, an original image is decomposed into three detail coefficients and one approximate coefficients. The decomposition can be recursively applied to the approximate image to generate a lower resolution of the pyramid. The segmentation starts at the lowest resolution using the K-means clustering scheme and the result is propagated through the pyramid to a higher one with continuously improving the segmentation. Results based on this method using 5\*5 and 7\*7 feature windows is showed in Fig.3.(b) and Fig.4.(b). Compared with Salari E's method, the proposed algorithm obtains the number of clusters automatically by finding the centers of the densest regions in the feature space. It succeeds in segmenting SAR images without any prior knowledge. On the other hand, using undecimated wavelet coefficients as features, Salari E's method can catch images' texture information, but K-means cluster can only generate spherical boundaries. Our method can avoid this drawback and delineate arbitrarily shaped of clusters.

We also using traditional mean shift approach obtain another team of results, Fig.3.(c) and Fig.4.(c). The traditional mean shift algorithm can delineate arbitrarily shaped clusters but can not performance well just using gray-level as features. Consequently, we can see that some parts of boundaries in our method's results are much more distinct than the other two's. Our method succeeds in overcoming the inherent limitations of methods based on undecimated wavelet features and feature clustering which always oversegment SAR image.

Here, we present a novel image segmentation algorithm, including three parts: extracting features using undecimated wavelet decomposition; selecting suitable feature subset by SFS algorithm; filtering feature subset using a Kuwahara filter; at last, applying mean shift algorithm to gain final results. In our method, prior knowledge of the number of clusters is not necessary as those classical algorithm., and clusters' shapes are not constrained.

Experiments demonstrated that the proposed method leads to a successful unsupervised segmentation. Compared with traditional meanshift segmentation and FCM based segmentation using undecimated wavelet decomposition, our algorithm had higher performance.

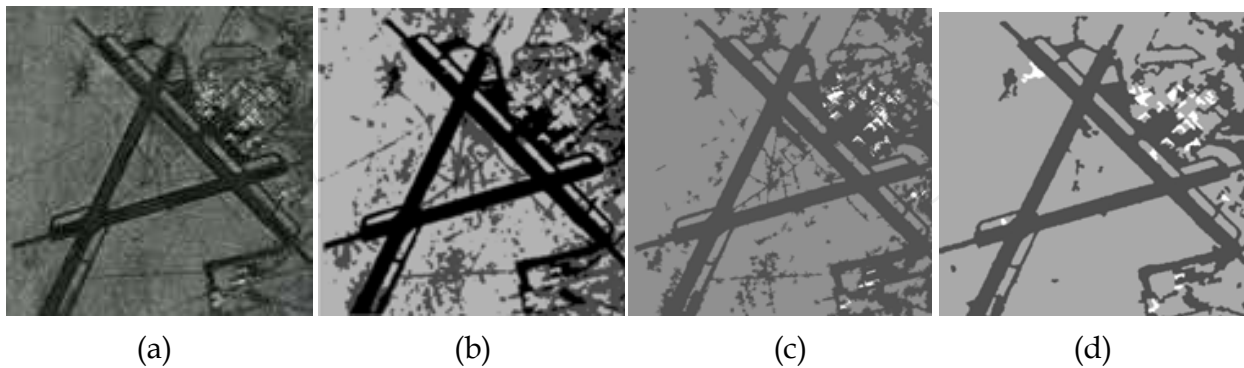


Fig. 3. 512\*512 SAR image segmented by different algorithms. (a) Original image, (b) Segmentation result using Salari E's method, (c) Segmentation result using mean shift, (d) Segmentation result using proposed algorithm.

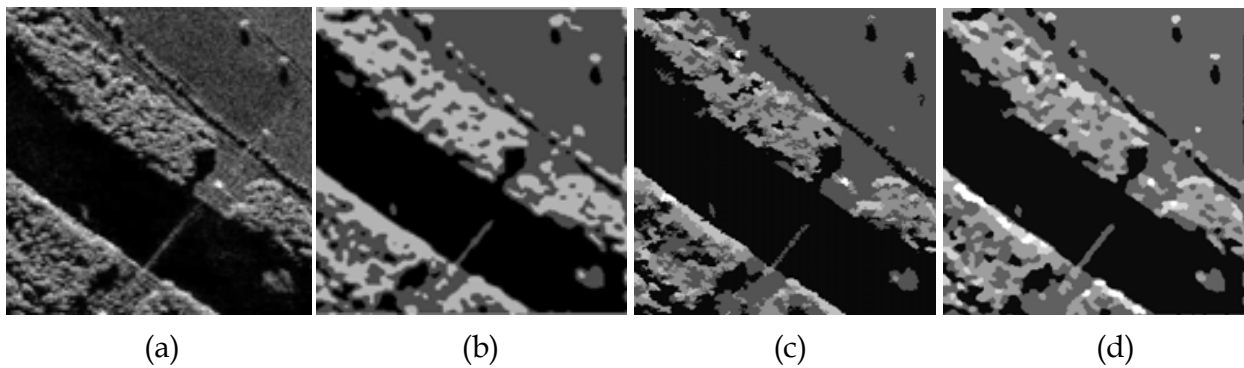


Fig. 4. 256\*256 SAR image segmented by different algorithms. (a) Original image, (b) Segmentation result using Salari E's method, (c) Segmentation result using mean shift, (d) Segmentation result using proposed algorithm.

#### 4. References

- [1] M. Kass and A. Witkin, "Snakes: Active Contour Models", *International Journal of Computer Vision*, 1(4), 321-331(1988).
- [2] C. Xu and J.L. Prince, "Snakes, Shapes, and Gradient Vector Flow", *IEEE Transactions on Image Processing*, 7(3), 359-369(1998).
- [3] Z. Yu and C. Bajaj, "Image Segmentation Using Gradient Vector Diffusion and Region Merging", *Proceedings of 16th International Conference on Pattern Recognition (ICPR'02)*, 941-944(2002).
- [4] C. Xu and J.L. Prince, "Gradient Vector Flow: A New External Force for Snakes", *Proceedings of IEEE Conference on Computer Vision and Pattern Recognition (CVPR'97)*, 66-71(1997).

- [5] S. Osher and J. A. Sethian, "Fronts Propagating with Curvature Dependent Speed: Algorithms Based on Hamilton- Jacobi Formulations", *Journal of Computational Physic*, 79(1), 12-49(1988).
- [6] R. Malladi and J.A. Sethian, "Shape Modeling with Front Propagation: A Level Set Approach", *IEEE Transactions on Pattern Analysis and Machine Intelligence*, 17(2), 158-175(1995).
- [7] P. Lin and C.X. Zhen, "Model-based Medical Image Segmentation: A Level Set Approach", *Proceedings of the 5<sup>th</sup> World Congress on Intelligent Control and Automation*, 5541-5544(2004).
- [8] I.B. Ayed and C. Vazquez, "SAR Image Segmentation with Active Contours and Level Set", *International Conference on Image Processing (ICIP)*, 2717-2720(2004).
- [9] K. Wang and C. A. Taylor, "Level Set Methods and MR Image Segmentation for Geometric Modeling in Computational Hemodynamics", *Proceedings of the 20<sup>th</sup> Annual International Conference of the IEEE Engineering in Medicine and Biology Society*, 20(6), 3079-3082(1998).
- [10] H.F. Du and L.C. Jiao "Clonal Operator and Antibody Clone Algorithms", *Proceeding of the First International Conference on Machine Learning and Cybernetics*, 506-510(2002).
- [11] J. Lie and M. Lysaker "A Binary Level Set Model and Some Applications to Mumford-Shah Image Segmentation", *IEEE Transactions on Image Processing*, 15(5), 1171-1181(2006).
- [12] T. F. Chan and L. A. Vese, "Active Contours Without Edges", *IEEE Transactions on Image Processing*, 10(2), 266-277(2001).
- [13] S. Beucher and F. Meyer, "The morphological approach to segmentation: The watershed transformation," in *Mathematical Morphology in Image Processing*, E. Dougherty, Ed. New York: Marcel Dekker,1992.
- [14] A. Bleau and L. J. Leon, "Watershed-based segmentation and region merging," *CVIU*, vol. 77, no. 3, pp. 317-370, Mar. 2000.
- [15] R. Adams and L. Bischof, "Seeded region growing," *Pattern Anal. Mach. Intell.*, vol. 16, no. 6, pp. 641-647, Jun. 1994.
- [16] J. Fan, G. Zeng, M. Body, and M. S. Hacid, "Seeded region growing: An extensive and comparative study," *PRL*, vol. 26, no. 8, pp. 1139-1156, 2005.
- [17] Pierre Soille. *Morphological image analysis (Second Edition)* [M].springer Verlag, 2002. 277 - 281
- [18] O. Lezoray and H. Cardot, "Bayesian marker extraction for color watershed in segmenting microscopic images," in *Proc. 16th Int. Conf. Pattern Recognition*, 2002, pp. 739-742.
- [19] O. Lezoray and H. Cardot, "Cooperation of color pixel classification schemes and color watershed: A study for microscopic images," *IEEE Trans. Image Process.*, vol. 11, no. 7, pp. 783-789, Jul. 2002.
- [20] Ilya Levner and Hong Zhang "Classification-Driven Watershed Segmentation" *IEEE TRANSACTIONS ON IMAGE PROCESSING*, VOL. 16, NO. 5, MAY 2007 1437-1445
- [21] F. Bergholm, "Edge focusing," *IEEE Trans. Putt Anal. Mach. Intellig.* vol. PAMI-9, pp. 726-741, Nov. 1987.
- [22] D. Marr and E. Hildreth, "Theory of edge detection," *Proc. of the Royal Society London B*, vol. 207, pp. 187-217, 1980.

- [23] Gonzalez C R, Woods R E. Digital Image Processing(Second Edition)[M]. Publishing House of Electronics Industry, 2002.
- [24] Otsu N. A threshold selection method from gray-level histogram [J]. IEEE Trans SMC, 1979, 9(1):62-66.
- [25] C. Lantuéjoul, "La Squelettisation et son Application aux Mesures Topologiques des Mosaiques Polycristalines," Ph.D. dissertation, School of Mines, Paris, France, 1978.
- [26] S. Beucher and F. Meyer, "The morphological approach to segmentation: the watershed transformation," in Mathematical Morphology and its Applications to Image Processing, E.R. Dougherty, Ed. New York: Marcel Dekker, 1993, ch. 12, pp. 433-481.
- [27] L. Vincent and P. Soille, "Watersheds in digital spaces: an efficient algorithm based on immersion simulations," IEEE Trans. Pattern Anal. Machine Intell., vol. 13, no. 6, pp. 583-598, 1991.
- [28] M. Petrou, L. Shafarenko, and J. Kittler, "Automatic watershed segmentation of randomly textured color images," IEEE Trans. Image Processing, vol. 6, pp. 1530-1544, Nov. 1997.
- [29] "Unsupervised Multiscale Color Image Segmentation Based on MDL Principle", IEEE, 2006
- [30] Dorin Comaniciu, Peter Meer, "Mean Shift: A Robust Approach Toward Feature Space Analysis", IEEE transactions on pattern analysis and machine intelligence, vol.24, NO.5, May 2002, 603~619.
- [31] Christopher, "Synergism in low level vision"
- [32] Richard O. Duda, Peter E. Hart, David G. Stork. Pattern Classification[M]. Li H D, Yao T X, Beijing: China Machine Press, 2003:132-164
- [33] Dorin Comaniciu, Peter Meer, "Mean Shift Analysis and Application"
- [34] J.-L. Starck, J. Fadili, "The Undecimated Wavelet Decomposition and its Reconstruction", 2006
- [35] Salari E, Ling Z. Texture segmentation using hierarchical wavelet decomposition [J]. Pattern Recognition, 1995, 28(12): 1819-1824.

IntechOpen



## **Recent Hurricane Research - Climate, Dynamics, and Societal Impacts**

Edited by Prof. Anthony Lupo

ISBN 978-953-307-238-8

Hard cover, 616 pages

**Publisher** InTech

**Published online** 19, April, 2011

**Published in print edition** April, 2011

This book represents recent research on tropical cyclones and their impact, and a wide range of topics are covered. An updated global climatology is presented, including the global occurrence of tropical cyclones and the terrestrial factors that may contribute to the variability and long-term trends in their occurrence. Research also examines long term trends in tropical cyclone occurrences and intensity as related to solar activity, while other research discusses the impact climate change may have on these storms. The dynamics and structure of tropical cyclones are studied, with traditional diagnostics employed to examine these as well as more modern approaches in examining their thermodynamics. The book aptly demonstrates how new research into short-range forecasting of tropical cyclone tracks and intensities using satellite information has led to significant improvements. In looking at societal and ecological risks, and damage assessment, authors investigate the use of technology for anticipating, and later evaluating, the amount of damage that is done to human society, watersheds, and forests by land-falling storms. The economic and ecological vulnerability of coastal regions are also studied and are supported by case studies which examine the potential hazards related to the evacuation of populated areas, including medical facilities. These studies provide decision makers with a potential basis for developing improved evacuation techniques.

### **How to reference**

In order to correctly reference this scholarly work, feel free to copy and paste the following:

Shuang Wang (2011). Segmentation Methods for Synthetic Aperture Radar, Recent Hurricane Research - Climate, Dynamics, and Societal Impacts, Prof. Anthony Lupo (Ed.), ISBN: 978-953-307-238-8, InTech, Available from: <http://www.intechopen.com/books/recent-hurricane-research-climate-dynamics-and-societal-impacts/segmentation-methods-for-synthetic-aperture-radar>

**INTECH**  
open science | open minds

### **InTech Europe**

University Campus STeP Ri  
Slavka Krautzeka 83/A  
51000 Rijeka, Croatia  
Phone: +385 (51) 770 447  
Fax: +385 (51) 686 166  
[www.intechopen.com](http://www.intechopen.com)

### **InTech China**

Unit 405, Office Block, Hotel Equatorial Shanghai  
No.65, Yan An Road (West), Shanghai, 200040, China  
中国上海市延安西路65号上海国际贵都大饭店办公楼405单元  
Phone: +86-21-62489820  
Fax: +86-21-62489821

© 2011 The Author(s). Licensee IntechOpen. This chapter is distributed under the terms of the [Creative Commons Attribution-NonCommercial-ShareAlike-3.0 License](#), which permits use, distribution and reproduction for non-commercial purposes, provided the original is properly cited and derivative works building on this content are distributed under the same license.

IntechOpen

IntechOpen